

New tools for electromechanical characterisation of piezoceramics

G. Feuillard · E. Le Clezio · F. Levassort ·
L. P. Tran Huu Hue · T. Delaunay · M. Lethiecq

Received: 15 March 2006 / Accepted: 14 May 2007 / Published online: 13 June 2007
© Springer Science + Business Media, LLC 2007

Abstract This paper presents three methods that can be used to characterise piezoelectric integrated structures or materials, based on the resolution of an inverse problem. Analytical models that describe the electrical and/or mechanical behaviour of the material or structure as a function of piezoelectric properties are developed, and the appropriate measurements are carried out on the piezoelectric materials. The fitting of these models with experimental data allows the piezoelectric properties to be determined. Three characterisation methods are described. The first one is based on the electrical impedance measurement of piezoelectric integrated structures. The second one, purely acoustic, is based on the measurement of transmission coefficients of a plane wave through a piezoelectric plate. The third method uses the principle of resonance ultrasound spectroscopy of a piezoelectric cube combined with Laser detection.

Keywords Piezoelectric materials · Characterisation methods · Tensorial properties

1 Introduction

Transduction phenomenon in the MHz range is mainly realised by means of piezoelectric materials, such as ferroelectric lead zirconate titanates. The materials requirements

for new ultrasonic transducer applications have brought materials research and device development closer together. During the last two decades, this has led to the design of materials such as lead free compositions [1], ternary compositions [2], single crystals [3, 4] or textured ceramics [5]. In particular, these new materials are developed for their integration in high sensitivity broadband medical imaging [6–8] and non-destructive testing transducers. This research also leads to the development and the optimisation of new processes such as thin or thick film production [9]. In this case, the piezoelectric material fabrication is directly integrated into the manufacturing of the ultrasonic probe [10–12]. This general tendency requires the development of accurate electromechanical characterisation tools. Indeed, measurement standards [13] are not available for all the variety of sample shapes and sizes and for the complex structures that have to be manufactured for transducer applications. Furthermore, numerical and analytical models of complex integrated structures require the full complex piezoelectric tensor.

In this paper, several measurement techniques developed to characterise piezoelectric materials and structures are presented. The first method is based on harmonic measurements of the electrical impedance of a sample. Characterisation of thick films and single crystals are reported using this technique. The second method uses the measurement of transmission coefficient of an ultrasonic plane wave through a piezoelectric plate as a function of frequency and angle. The full tensor characterisation of a PZT piezoelectric plate is reported and compared with characterisations using other methods. Finally, preliminary results on the implementation of the spectroscopic resonance method applied to a piezoelectric cube for full tensor characterisation are presented.

G. Feuillard (✉) · E. L. Clezio · F. Levassort · L. P. T. H. Hue ·
T. Delaunay · M. Lethiecq
Université François-Rabelais,
LUSSI FRE CNRS 2448, ENIVL rue de la Chocolaterie,
41034 Blois Cedex, France
e-mail: gfeuillard@univ-tours.fr

2 Characterisation based on electrical measurements

2.1 Integrated structures

In the case of integrated structures such as thick films laid down on a substrate (Fig. 1), the thickness mode electro-mechanical properties can no longer be directly deduced from electrical measurements on a free resonator [13]. If lateral dimensions of the sample are large enough compared to the thickness, the harmonic vibration of the structure can be modelled using one dimensional electroacoustic models such as KLM model [13, 14]. If passive elements of the device are known, the thickness mode piezoelectric properties can be deduced from electrical impedance measurements by fitting the input parameters of the KLM electroacoustic model to experimental data [7, 15].

An illustration of this technique is given in the case of Navy type I piezoelectric ceramic PZT thick film (PZ26 manufactured by Ferroperm Piezoceramics) laid down on silicon substrate (Fig. 2).

The film has dimensions of $8 \times 8 \times 0.06 \text{ mm}^3$; it has electrodes on both faces with respectively a $3 \text{ }\mu\text{m}$ thick bottom gold electrode, a $0.5 \text{ }\mu\text{m}$ thick platinum barrier layer and a $5 \text{ }\mu\text{m}$ thick top silver electrode. Measurements were carried out on an Agilent 4395A analyser. The fitted parameters are the density, the longitudinal wave velocity, the dielectric constant, the thickness coupling factor and the dielectric and mechanical loss tangents. The fitting procedure operates not only on a narrow bandwidth (Fig. 2a) but also on a large frequency span that includes many harmonic vibrations of the structure [Fig. 2(b)]. As already noticed, the knowledge of the substrate and electrodes mechanical properties is crucial for accurate determination of electro-mechanical properties of the thick film. Electromechanical properties of the sample deduced from the fitting procedure are given in Table 1.

Here, due to fabrication process, the density, the dielectric constant and the velocity of the material are lower than those of conventional bulk PZ26. Nevertheless, the thickness coupling coefficient of 42% shows that the structure shows good piezoelectric activity, which is suitable for ultrasonic transducer applications.

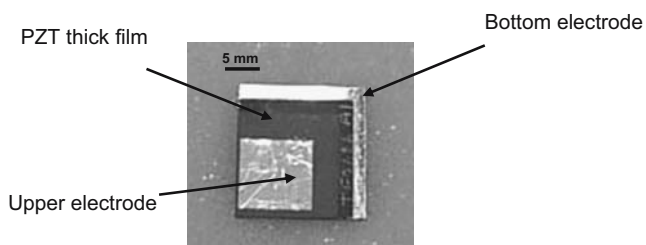


Fig. 1 PZT thick film laid down on silicon substrate

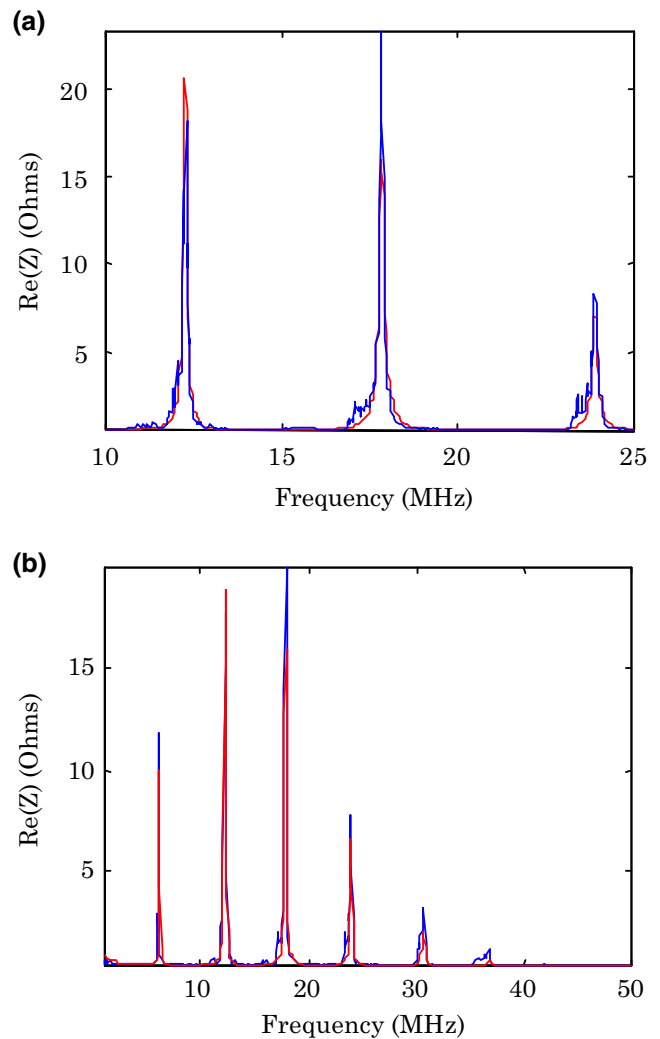


Fig. 2 Real part of the electrical input impedance of PZ26 thick film laid down on silicon substrate for two frequency ranges (*blue*: experimental, *red*: theoretical). (a) Comparison experiment theory on a narrow bandwidth. (b) Comparison experiment theory on a large bandwidth

Table 1 Electromechanical properties of PZ26 thick film.

| | Thick film material, Pz26 | Substrate, Si (001) |
|-----------------------------|---------------------------|---------------------|
| ρ (kg/m ³) | 5,425 | 2,340 (fixed) |
| ϵ_{33r}^S | 335 | |
| V_l (m/s) | 3,190 | 8,430 (fixed) |
| K_t (%) | 42 | |
| δ_m (%) | 2.2 | |
| δ_e (%) | 1 (fixed) | |
| Z (Mra) | 17.3 | |
| F_0 (MHz) | 26.6 | |
| Thickness (μm) | | 500 (fixed) |
| Z_s (Mra) | | 19.7 (fixed) |

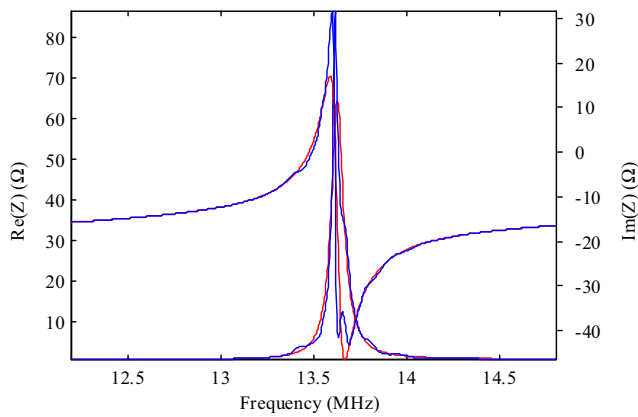


Fig. 3 Real part of the electrical input impedance of PZN-4.5PT single crystal around the third harmonic (blue: experimental, red: theoretical)

2.2 Frequency characterisation

This fitting procedure can also be used to examine the frequency behaviour of electromechanical properties of piezoelectric materials [16, 17]. To quantify this evolution with frequency, the characterisation process using a fitting method is performed at each electrical resonance. This procedure was applied to PZN-xPT ($4.5 < x < 12$) single crystals. Figure 3 shows the result of the fit procedure on the third harmonic of the electrical impedance of a PZN-4.5PT single crystal.

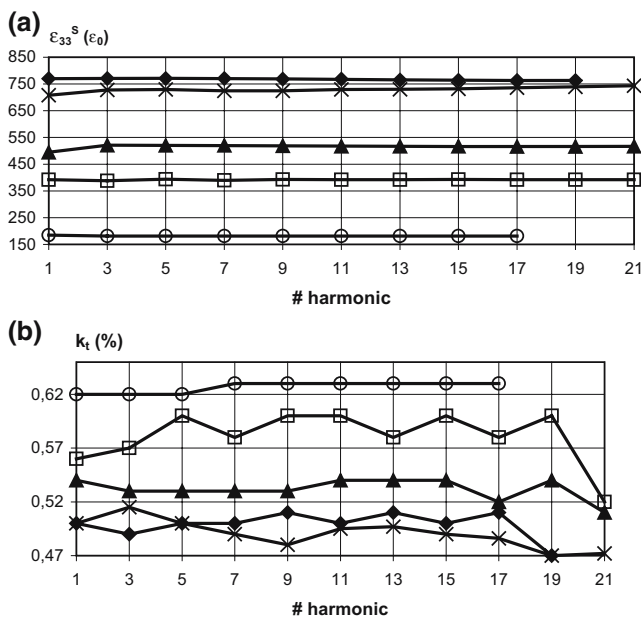


Fig. 4 (a) Relative dielectric constant of PZN-xPT ($4.5 < x < 12$) single crystal versus the harmonic number. (b) Thickness coupling factor of PZN-xPT ($4.5 < x < 12$) single crystal versus the harmonic number. —×— PZN-4.5PT, —◆— PZN-7PT, —▲— PZN-8PT, —□— PZN-9PT (Mn), —○— PZN-12PT

Here again, the fitted parameters are the velocity, the dielectric constant, the thickness coupling factor and the dielectric and mechanical loss tangent. The high frequency properties of the piezoelectric material can then be evaluated from measurements on a bulk sample. Figure 4(a, b) present the thickness coupling factors and dielectric constant of PZN-xPT single crystal versus the harmonic number. Here the harmonic #21 corresponds to a frequency around 90 MHz in all cases, except for the Mn doped PZN-9PT where it corresponds to 50 MHz.

For high frequency characterisations, these results have been compared to electromechanical characterisations on thin plates. In the case of PZN-7PT, the reduction in thickness has a large effect on electromechanical properties (Table 2). The dielectric constant increases about 25% when the plate thickness decreases from 440 to 80 μm . This result can be correlated with the increase of the electrical loss tangent. Both results suggest that the conductivity of the material increases when the thickness decreases. Here, the charged-domain-walls have possibly a strong influence on the change of properties. When a thick sample is considered, the probability for electrons to go from one side to another is far lower than for thin samples which explain both the increase of the electric loss tangent and dielectric constant.

3 Tensorial characterisation based on the measurement of acoustic wave transmission coefficients

Very often, when numerical tools (such as Finite Element Methods) or complex analytical models are developed, the thickness mode properties of the piezoelectric material are no longer sufficient to predict the behaviour of ultrasonic transducers or piezoelectric devices. The full piezoelectric tensor is then required for modelling. A tensorial characterisation can be carried out using the IEEE standard on piezoelectricity [13] or derivative methods that require several samples [18]. Mixed methods that combine electrical and ultrasonic measurements have also been investigated

Table 2 Electromechanical properties of a PZN-7PT measured for various thickness.

| Properties | | | |
|--------------------------------------|-------|-------|-------|
| Thickness (μm) | 440 | 200 | 80 |
| Lateral dimensions (mm^2) | 100 | 22.8 | 1.73 |
| Fundamental resonance (MHz) | 4.6 | 10.8 | 24.2 |
| ϵ_{33r}^S | 771 | 870 | 1,131 |
| V_1 (m/s) | 4,060 | 4,006 | 3,970 |
| K_t (%) | 0.49 | 0.47 | 0.38 |
| δ_m (%) | 0.35 | 5.4 | 3 |
| δ_e (%) | 5 | 0.34 | 7.9 |

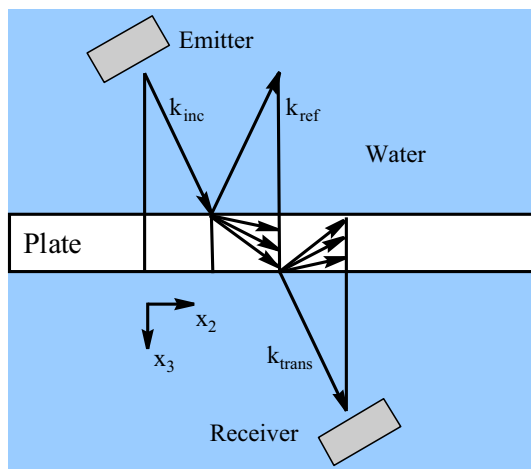


Fig. 5 Principle of transmission coefficient measurement

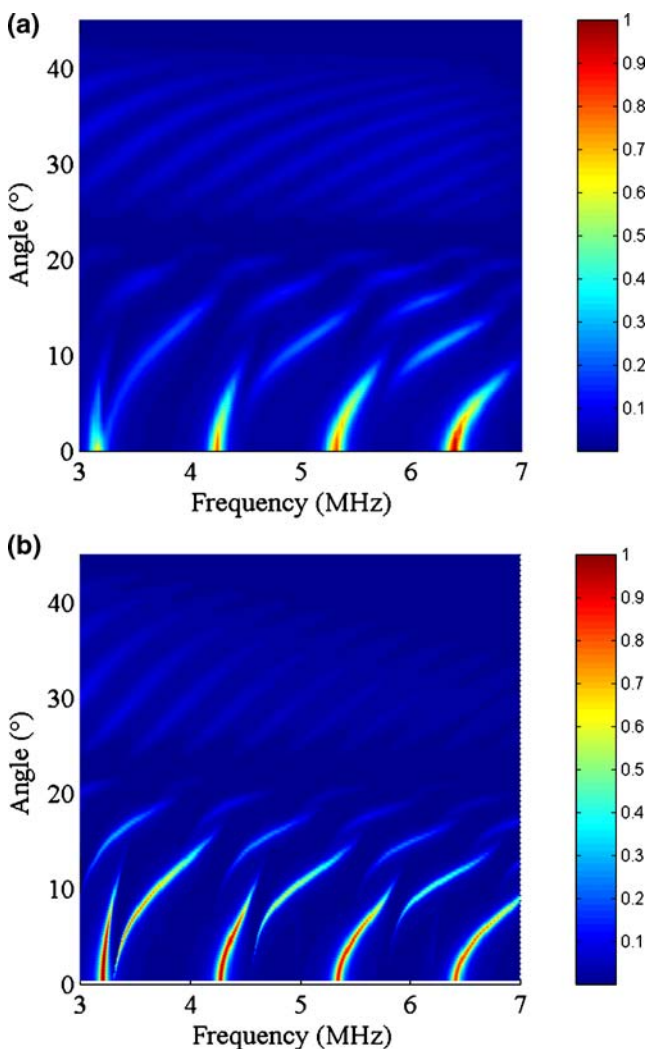


Fig. 6 Experimental (a) and theoretical (b) transmission coefficients through a soft PZT plate (PZ27 manufactured by Ferroperm Piezoceramics)

[19]. However, a major drawback of these methods is that they require samples of various shapes and size which means that the sample preparation has a strong influence on the reliability of the characterisation. In particular, shear mode piezoelectric samples are known to be difficult to prepare, and consistency of the tensor is not guaranteed. Alternatively, the tensorial characterisation of anisotropic piezoelectric materials can be achieved using ultrasonic techniques [20–25]. The principle is to measure the transmission/reflection coefficient through a plate as a function of the incidence angle and frequency (Fig. 5).

For a given angle, an incident longitudinal plane wave generated by an ultrasonic transducer is transmitted to the plate. By mode conversion inside the plate, longitudinal and transverse waves are generated. On the other side, the receiving transducer will detect a signal that depends on the plate material properties. These measurements of the transmission coefficients are then compared to a theoretical predictive model, the input of which is the piezoelectric tensor of the material. The treatment of the inverse problem gives the tensorial properties of the material [27]. In this case, the theoretical model for describing reflection-transmission of plane acoustic waves through piezoelectric anisotropic plates uses the octet formalism of piezoacoustics [20, 21] and the concept of the impedance/admittance [22–26] or stiffness/compliance matrices. A specific version of the admittance matrix has been introduced in a way to incorporate different types of electrical boundary conditions for an immersed plate [27]. Therefore, the reflection and transmission coefficients are expressed through this admittance in explicitly the same way as in the case of a pure elastic plate.

This method was applied to the characterisation of a soft PZT plate (PZ27 manufactured by Ferroperm Piezoceramics) with dimensions $79.8 \times 79.8 \times 2.025 \text{ mm}^3$. The sample is

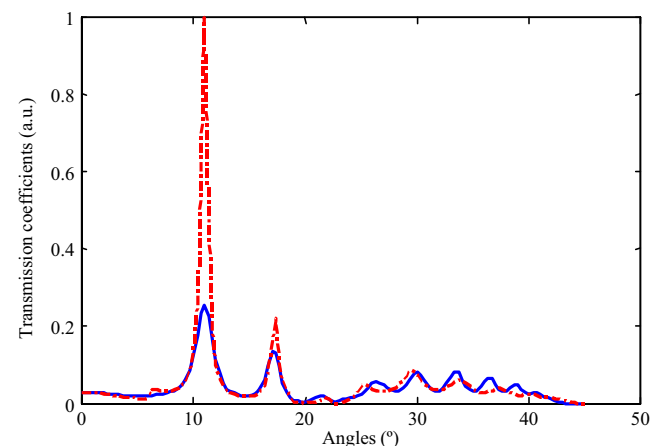


Fig. 7 Theoretical (red) and experimental (blue) transmission coefficient through PZ27 piezoelectric plate as function of the angle (frequency 5 MHz)

Table 3 Comparison of the material constants obtained by ultrasonic transmission measurements and provided by Ferroperm Piezoceramics (real parts).

| Property | Units | Fitted properties | Original data set |
|------------------------------|--------------------|----------------------|-------------------|
| Density | | | |
| ρ | kg m ⁻³ | 8,060 | 8,060 |
| Elastic rigidity | | | |
| C_{11}^E | GPa | 114.3–3.3 <i>i</i> | 147 |
| C_{12}^E | GPa | | |
| C_{13}^E | GPa | 72.3–0.7 <i>i</i> | 93.7 |
| C_{33}^E | GPa | 103.6–0.015 <i>i</i> | 113 |
| C_{44}^E | GPa | 20.3–0.016 <i>i</i> | 23 |
| C_{66}^E | GPa | | |
| Relative dielectric constant | | | |
| ϵ_{33}^S | – | 863+0.56 <i>i</i> | 914 |
| ϵ_{11}^S | – | 1,138+0.13 <i>i</i> | 1,130 |
| Piezoelectric constants | | | |
| e_{33} | C m ⁻² | 15.52 | 16 |
| e_{31} | C m ⁻² | –3.26 | –3.06 |
| e_{15} | C m ⁻² | 11.76 | 11.64 |

fixed on a motorised rotation stage and is immersed into a water tank. Both emitting and receiving transducers have an active diameter of 19.05 mm (Technisonic ILD-0506-HR) with a 5 MHz centre frequency that ensure the condition of plane wave generation and detection. The emitting transducer is excited by a burst of one sinusoidal period centred at 5 MHz. Every motorised stage is computer controlled. The transmitted acoustic fields are captured for an incident angle ranging from 0° to 45° every 0.3°. This leads to 136 captured signals. The reference signal transmitted through water without the sample has also been recorded. Fast Fourier Transform is then performed and the transmitted spectra are divided by the reference one, thus yielding the angular spectrum of the absolute value of transmission coefficient at a given frequency.

Figure 6 shows the experimental and theoretical transmission coefficients through a PZT plate. For a 0° incidence



Fig. 8 Experimental set-up

angle the transmission spectrum presents sharp resonances that correspond to length extensional modes in the plate. When the incidence angle increases, multiple transmission branches appear corresponding to a coupling of longitudinal and transverse modes at the interfaces of the plate. The elastic, piezoelectric and dielectric properties of the plate are inferred from fitting the numerical simulation with the experimental data obtained from the transmission measurements.

The fitting procedure was carried out using the simplex method that minimises the quadratic distance between model and experimental data. It was applied to the complex piezoelectric tensor of the material. It allows not only the accurate determination of resonance location but also reproduces the spreading of resonances due to attenuation (Fig. 7).

Table 3 shows a comparison between the data supplied by Ferroperm Piezoceramics [28] and the results obtained from both electrical admittance and ultrasonic transmission measurements. The largest difference with the manufacturer data is observed for the coefficients C_{11}^E and C_{13}^E which are notoriously difficult to characterise. However, the relative difference does not exceed 20% from the original data set, which is within the confidence interval given by the manufacturer. The real parts of the coefficients C_{13}^E , e_{33} and ϵ_{33}^S , identified by two different methods, are very close: the relative discrepancy is lower than 7%. Large differences, though, appear between the imaginary parts of these parameters. This may be related to the fact that the inhomogeneities of the sample broaden the resonances of the electrical measurements, leading to an overestimation of the attenuation in the material.

With this method, the effect of electrodes can also be examined by two means. First, a three-layer structure can be modelled, where the dielectric constants of the electrodes are set to infinity in order to represent a conductive material. However, if the electrodes are much thinner than the material, the specific version of the admittance matrix presented in [27] can model the electrodes simply by considering that the medium surrounding the plate is conductive.

4 Resonant ultrasound spectroscopy

Tensorial properties of materials can also be deduced from the study of the free vibrations of parallelepiped samples. The analysis presented by Desmarest [30] and Ohno [31] in the case of an orthorhombic crystal, was extended to piezoelectricity in the 1980s [31]. It is now being developed for material characterisation [32–34]. The theoretical approach is based on the formulation of the Lagrangian of an electroelastic body [30]. The eigen values and vectors of

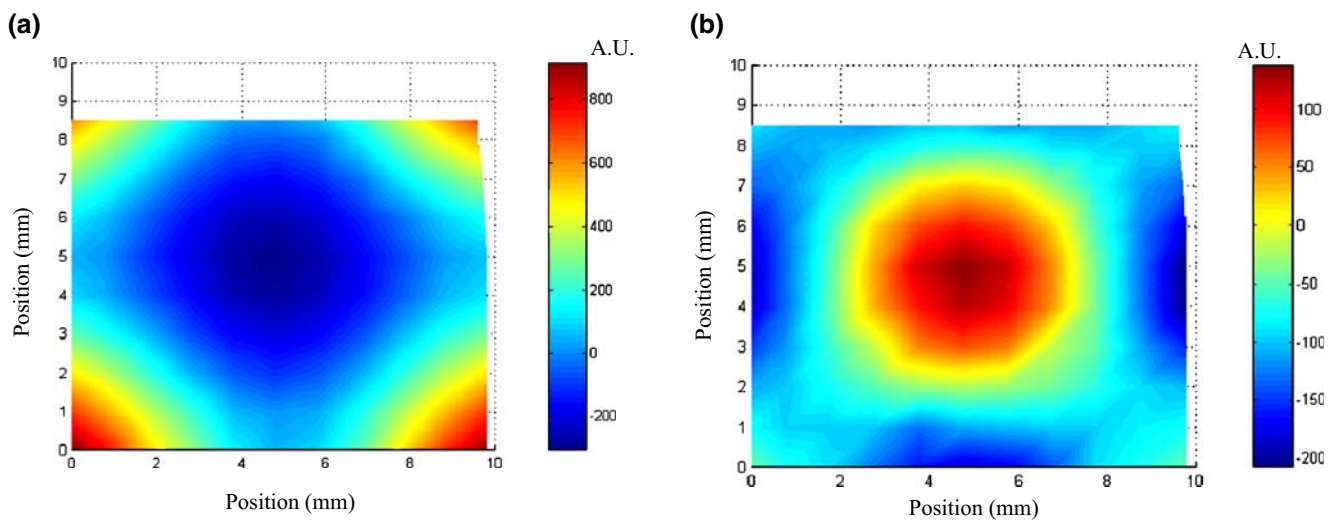


Fig. 9 Experimental normal displacement fields on the surface of a PMN-35PT cube. (a) Resonant frequency 176.0 kHz, (b) resonant frequency 241.3 kHz

the Lagrangian correspond to the free resonance frequencies and displacements. The basis functions that approximate the exact solution for the vibration of an elastic body can be arbitrarily selected. However, it is well-known that the Legendre polynomial basis minimises the degree of the polynomials used to approximate the free mechanical vibration of parallelepipeds. Mechanical resonant frequencies of a piezoelectric body depend on the complete piezoelectric tensor $C_{\alpha\beta}^E$, $e_{i\alpha}$ and ε_{ij}^S . Resonant ultrasound spectroscopy can be used and the treatment of the inverse problem yields the desired coefficients. A difficulty of the method when applied to a piezoelectric material is that the contributions of the piezoelectric and dielectric coefficients to the mechanical vibrations are very small. In most cases the sample is sandwiched between two transducers, which limits the measurement bandwidth to that of the transducers. To avoid this limitation, a mixed electrical generation/laser detection method is developed for the characterisation of materials (Fig. 8). A piezoelectric cube metalised on two faces is placed on the impedance test clip fixture of an Agilent 4395A impedance analyser. This analyser is used as a broadband excitation source to generate free resonances in the cube and to visualise its electrical input impedance. A Polytech laser interferometer is used to detect the displacement field in the normal direction. Displacement cartography is obtained with the aid of a XY automated translation unit on which the test clip fixture is mounted.

First measurements were performed on a PMN-35PT piezoceramic manufactured by Thales Research Technology with dimensions $10 \times 10 \times 10 \text{ mm}^3$. Natural frequencies of the thickness mode are typically comprised between 100 and 200 kHz.

Figure 9 shows the experimental displacement fields measured with the laser interferometer for two resonances. The XY cartography was obtained with steps of 1 mm which leads to a hundred measurements on the sample. Experimental resonances are respectively 176.0 and 241.3 kHz for these two vibration modes.

The fitting procedure was performed on resonant frequencies of the cube step by step. First, pure modes that only involve shear or longitudinal coefficients are selected, characterised and the associated piezoelectric coefficients are deduced. Then, when selecting other vibration modes, these parameters are fixed and other properties are adjusted using

Table 4 Elastic, piezoelectric, and dielectric properties of PMN-35PT ceramics.

| Property | Units | Fitted properties | Original data set [34] |
|------------------------------|--------------------|-------------------|------------------------|
| Density | | | |
| ρ | kg m^{-3} | 8,060 | 8,060 |
| Elastic rigidity | | | |
| C_{11}^E | GPa | 175 | 168.80 |
| C_{12}^E | GPa | 117 | 116.83 |
| C_{13}^E | GPa | 119 | 116.80 |
| C_{33}^E | GPa | 155 | 154.43 |
| C_{44}^E | GPa | 28 | 30.56 |
| C_{66}^E | GPa | 29 | 25.97 |
| Relative dielectric constant | | | |
| ε_{33}^S | – | 2,825 | 2,622 |
| ε_{11}^S | – | 2,373 | 2,367 |
| Piezoelectric constants | | | |
| e_{33} | C m^{-2} | 27.0 | 30.15 |
| e_{31} | C m^{-2} | –6.5 | –6.92 |
| e_{15} | C m^{-2} | 15.0 | 16.66 |

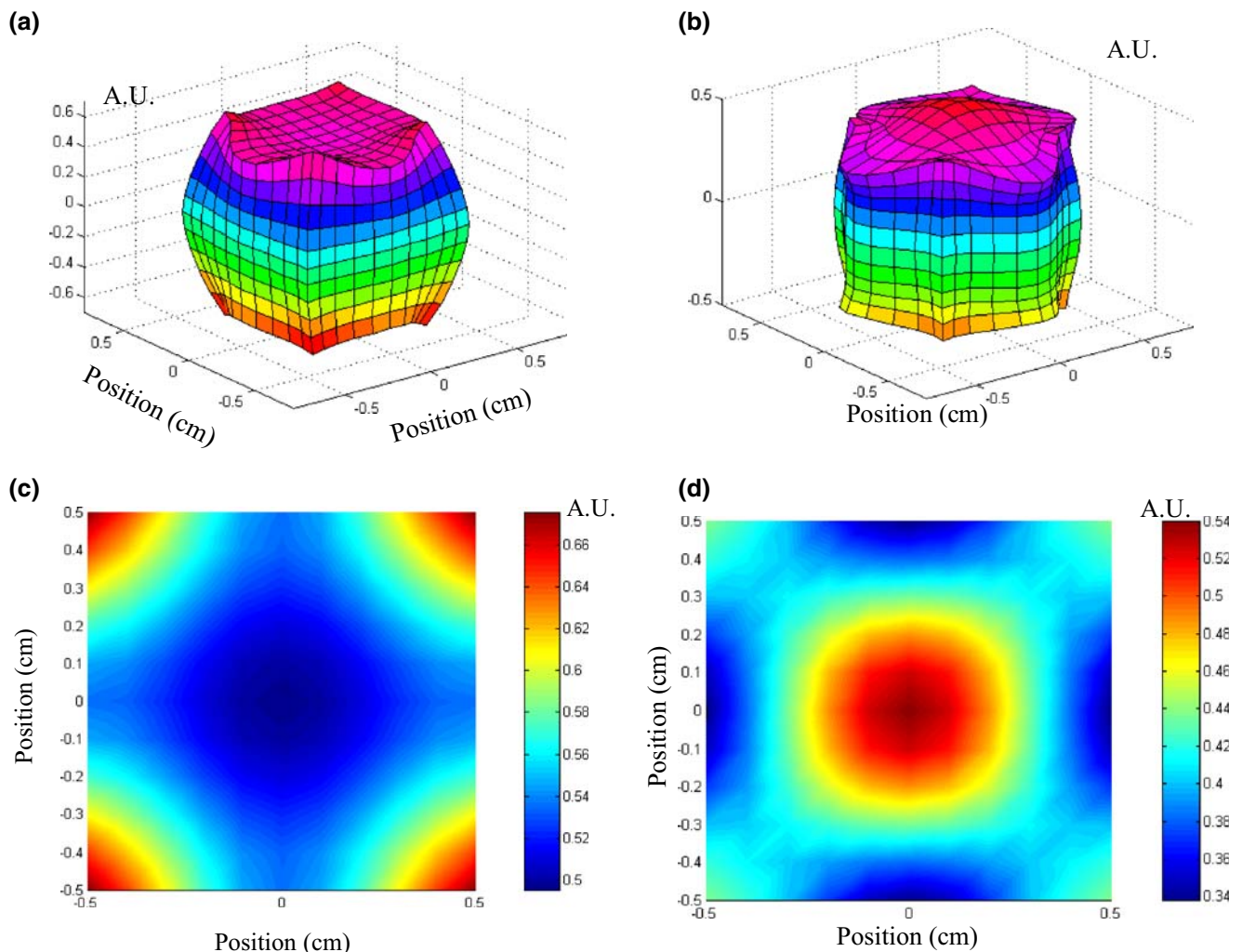


Fig. 10 Theoretical displacement fields of PMN-35PT piezoceramic. (a, b) Resonant frequency 176.6 kHz, (c, d) resonant frequency 246.6 kHz

the fitting procedure. In this way, the number of unknowns at each fitting stage is lower than the total number of unknowns. Theoretical displacements were calculated from fitted piezoelectric properties given in Table 4 and are represented in Fig. 10. The first mode presented [Fig 10(a, b)] mainly involves longitudinal vibrations with main displacement at the centre of the cube. The second mode [Fig. 10(c, d)] of higher frequency has a more complex shape that involves the complete piezoelectric tensor. The two theoretical natural resonance vibrations associated are respectively 176.6 and 246.6 kHz. Comparison of theoretical displacement fields with experimental results (Fig. 10) leads to a very good agreement on these two vibration modes.

The fitted tensor obtained from resonant ultrasound spectroscopy is close to that obtained from previous characterisations of this material [35] (Table 4). Relative deviations do not exceed 10%. These results show that this method can be applied to tensorial characterisation of piezoceramics.

5 Conclusion

The development of new characterisation methods for piezoelectric materials and structures is major importance for the development on new compositions and devices. The variety of structures and shapes encountered do not allow the use of the standard methods for piezoelectric characterisation. These functional properties are not only required to model the electroacoustic behaviour of integrated structures or devices, but are also useful to material developers. Starting from a direct problem of modelling of a piezoelectric material, the treatment of the inverse problem allows the material to be characterised. Three characterisation methods that take into account sample geometry were proposed. In a first method, the material properties were determined from the electrical impedance measurement of the piezoelectric structure. This technique is particularly adapted to thick film characterisation and investigating the effect of frequency. The second method

consists of measuring the transmission coefficient of an ultrasonic plane wave through a piezoelectric plate. It allows full tensor determination to be achieved. It can be extended to multi-layered structures and composite materials. Finally, the resonant ultrasound spectroscopy of a cube combined with laser measurement also enables the determination of full piezoelectric tensor. Furthermore, it offers the possibility of using small sized samples as the measurement area is directly related to the laser spot size, which is few tenths of μm .

Acknowledgement This work was performed within the European MIND Network of Excellence and MINUET Strep projects (6th Framework Programme) and supported by the French Ministry of Research through RNTS project DEMOCRITE.

References

1. Y. Saito, H. Takao, T. Tani, T. Nonoyama, K. Takatori, T. Homma, T. Nagaya, M. Nakamura, *Nature* **432**, 84 (2004)
2. H. Wang, B. Jiang, T. R. Shrout, W. Cao, *IEEE Trans. Ultrason. Ferroelectr. Freq. Control* **51**, 908 (2004)
3. R. Zhang, B. Jiang, W. Cao, *J. Appl. Phys.* **90**, 3471 (2001)
4. W. Jiang, R. Zhang, B. Jiang, W. Cao, *Ultrasonics* **41**, 55 (2003)
5. T. Kimura, Y. Sakuma, M. Murata, *J. Eur. Ceram. Soc.* **25**, 2227 (2005)
6. N. Felix, L.P. Tran-Huu-Hue, L. Walker, C. Millar, M. Lethiecq, *Ultrasonics* **38**, 127 (2000)
7. L.P. Tran-Huu-Hue, F. Levassort, N. Felix, D. Damjanovic, W. Wolny, M. Lethiecq, *Ultrasonics* **38**, 219 (2000)
8. K.C. Cheng, H.L.W. Chan, C.L. Choy, Q. Yin, H. Luo, *IEEE Trans. Ultrason. Ferroelectr. Freq. Control* **50**, 1177 (2003)
9. C. Chao, Z. Wang, W. Zhu, *Thin Solid Films* **493**, 313 (2005)
10. Y.S. Yoon, S.H. Kim, S.J. Lee, H.K. Kim, M.J. Lee, *Sens. Actuators A* **125**, 463 (2006)
11. Z. Wang, W. Zhu, J. Miao, H. Zhu, C. Chao, O.K. Tan, *Sens. Actuators A* **130**, 485–490 (2006)
12. P. Maréchal, F. Levassort, J. Holc, L.P. Tran-Huu-Hue, M. Kosec, M. Lethiecq, *Proceedings of 2005 IEEE Ultrasonic Symposium*, 2223 (2005)
13. European standard, EN 50324–2:2002
14. R. Krimholtz, D.A. Leedom, G.L. Matthei, *Electron. Lett.* **38**, 398 (1970)
15. S.J.H. Van Kervel, J.M. Thijssen, *Ultrasonics* **21**, 134 (1983)
16. F. Levassort, L.P. Tran Huu Hue, J. Holc, T. Bove, M. Kosec, M. Lethiecq, *Proceedings of 2001 IEEE Ultrasonic Symposium*, 1035 (2001)
17. M. Lethiecq, L.P. Tran-Huu-Hue, F. Patat, L. Pourcelot, *IEEE Trans. Ultrason. Ferroelectr. Freq. Control* **40**, 232 (1993)
18. T. Delaunay, E. Le Clezio, H. Dammak, P. Gaucher, M. Pham Thi, M. Lethiecq, G. Feuillard, *J. Phys. IV (France)* **128**, 161 (2005)
19. C. Alemany, A.M. Gonzalez, L. Pardo, B. Jiménez, F. Carmona, J. Mendiola, *J. Phys. D Appl. Phys.* **28**, 945 (1995)
20. W. Jiang, R. Zhang, B. Jiang, W. Cao, *Ultrasonics* **41**, 55 (2003)
21. J. Lothe, D.M. Barnett, *J. Appl. Phys.* **47**, 1799 (1976)
22. E.L. Adler, *IEEE Trans. Ultrason. Ferroelectr. Freq. Control* **37**, 485 (1990)
23. B. Honein, A.M. Braga, P. Barbone, G. Herrmann, *J. Intell. Mater. Syst. Struct.* **2**, 542 (1991)
24. V.Y. Zhang, J.-E. Lefebvre, C. Bruneel, T. Gryba, *IEEE Trans. Ultrason. Ferroelectr. Freq. Control* **48**, 1449 (2001)
25. V.Y. Zhang, T. Gryba, J.M. Orellana, B. Collet, *Acta Acustica* **88**, 218 (2002)
26. A.L. Shuvalov, O. Poncelet, M. Deschamps, *Wave Motion* **40**, 413 (2004)
27. A.L. Shuvalov, *Proc. R. Soc. Lond. A* **456**, 2197 (2000)
28. E. Le Clezio, A. Shuvalov, *Proceedings of 2004 IEEE Ultrasonic Symposium*, 553 (2004)
29. *Piezoelectric Materials Data Book*, Ferroperm, Kvistgaard, Denmark, (1996)
30. H.J. Desmarest, *J. Acoust. Soc. Am.* **49**, 768 (1971)
31. I. Ohno, *J. Phys. Earth* **24**, 355 (1976)
32. I. Ohno, *Phys. Chem. Miner.* **17**, 371 (1990)
33. H. Ogi, N. Nakamura, K. Sato, M. Hirao, S. Uda, *IEEE Trans. Ultrason. Ferroelectr. Freq. Control* **50**, 553 (2003)
34. H. Ogi, N. Nakamura, M. Hirao, H. Ledbetter, *Ultrasonics* **42**, 183 (2004)
35. H. Hemery—Céramiques orientées hautes performances : Pb (Mg1/3Nb2/3)O3-PbTiO3 par croissance interfaciale, Thèse de doctorat INSA Lyon, 12 décembre 2003